

# TMD's control effect on the nonlinear dynamic response of a barge FWOT

Elvidio. Gavassoni<sup>1</sup>, Paulo D. G. Zwierzikowski<sup>1</sup>

<sup>1</sup>*Prog. de Pós-Graduação em Eng. Civil, Universidade Federal do Paraná  
DCC/TC, Bloco III Caixa Postal 19011, 81531-980  
gavassoni@ufpr.br, paulognatta@gmail.com*

**Abstract.** The use of wind turbine is increasing all over the world. Floating support-platform configurations, such barge, are used at deep water conditions. The barge configuration achieves basic static stability in pitch and roll using a large waterplane area and shallow draft. Such structures can exhibit large displacements when vibrating which demands a nonlinear dynamic analysis. Passive structural control, such a tuned mass damper could be used in order to keep the structure stability. The main goal of this work is to investigate the effects of a tuned mass damper (TMD) upon the nonlinear oscillation of a barge-type floating offshore turbine. The analysis uses the nonlinear normal modes to obtain reduced order models of the system. The reduced order model results are compared to the numerical integration of the equations of motion and a good agreement between both results is found. The analytical obtained method is used to investigate important nonlinear phenomena such jumping and multiple coexisting solutions. A parametric TMD damping and mass ratio is performed in order to obtain their optimized values.

**Keywords:** vibration control, nonlinear normal modes, floating wind turbine, dynamic response, structural control.

## 1 Introduction

As a renewable energy source, offshore wind energy has been focus of many scientific studies and economic exploitation (Vis and Varsavas,[1]). Floating offshore wind turbines (FWOT) become economically more attractive than fixed ones when they are employed at deep water wind farms (Hu et al., [2]). As an example of floating platforms that can be used to support FWOT, the barge-type achieves basic static stability in pitch and roll using a large waterplane area and shallow draft (Collu et al., [3]). Combine large dimensions, high specific strength material and floating support, these slender structures (Zuo et al, [4]) barge FWOT could exhibits large displacement motion under the action of environmental forces such as winds, currents and waves. This excitation may impose to the FWOT tower considerable loads, which could suffer damage, fatigue and maintenance costs.

One approach to load mitigation is to use the structural control techniques to directly inhibit platform or tower vibration, where an auxiliary spring mass system adhered to the primary structure is commonly used. Such a device is known as tuned mass damper (TMD) (Li and Gao, [5]). In the lasty years many studies regarding the TMD performance at load mitigation and vibration suppress has be conducted on FWOTs (Stewart,[6]), including barge ones. Xi and co-workers [7] investigated a platform-based TMD, while He and co-workers [8] considered a tower-based one. Both studies consider the optimization of TMD parameters such as mass, stiffness and damping. A further modification was investigated by Sarkar and Fitzgerald [9], which have used a tuned mass-damper-inerter to reduce a spar FWOT vibration. However, these studies focused on the linearized systems. Linear analysis could fail to capture and describe important intrinsically nonlinear phenomena. A nonlinear dynamic analysis is, therefore, mandatory for a safe design of those structures. The use of models with a large number of degrees-of-freedom such as element finite schemes could be a very cumbersome task, mainly in parametric analysis and optimization studies. An alternative to overcome such difficulties is to use the nonlinear normal modes (NNMs) concept to obtain reduced order models of the problem (Gavassoni et al., [10]). Previously, the authors has been

showed that the NNMs could satisfactory be used to perform nonlinear analysis of FWOTs [11].

This work uses the nonlinear normal modes to derive a reduced order model of a wind turbine supported by an ITI Energy Barge 40 m x 40 m x 10 m barge with eight catenary mooring lines (Jonkman, [12]). Additionally, the structural responses of the wind turbine are mitigated by using a single-degree of freedom tower-based TMD with a elastic-linear stiffness coefficient. The Lagrange formulation is used to derive the nonlinear equations of motion of the FWOT-TMD system. The reduced order model (ROM) obtained by the use of the NNMs are used to study the forced vibrations of the problem. Some rich nonlinear dynamics phenomena are found such as multiple periodic solutions, node-saddle bifurcations, unstable solutions, jump and dynamic hysteresis. A parametric study on the TMD configuration is carried out to study its vibration suppression performance, resulting in optimized values;

## 2 Formulation

This study considers a National Renewable Energy Laboratory (NREL) 5-MW wind turbine, completely described by Jonkman and coworkers [13], supported by an ITI Energy barge floating platform whose description is given by Jonkman [12]. The barge-tower structure is modelled here using a 3-Degrees-of-freedom (DOF) rigid body model commonly used in the specialized literature ([2]; [6]; [7]; [8]; [11]; [14] and [15]) and showed in Fig. 1. The 3 DOF are: the barge pitch motion ( $\theta_B$ ); the tower fore-aft motion ( $\theta_T$ ) and the displacement of the TMD from the vertical axis  $z$  ( $x_{TMD}$ ). The tower is modelled as a rigid beam with a single lumped mass ( $m_T$ ) (considering the tower, nacelle and blades masses together) located at its center of mass distant  $L_T$  from the hinged point  $O$ . The tower-barge connection stiffness is modelled as a linear rotational spring of constant equal to  $k_T$ . The barge mass,  $m_B$ , is located at a distance  $L_B$  from the hinged point  $O$ . The restoring moments, given by mooring systems and buoyance, are modelled using a linear rotational spring of constant equal to  $k_B$ . The TMD mass,  $m_{TMD}$ , is located at a distance  $L_{TMD}$  from the hinged point  $O$  and has a linear stiffness coefficient equal to  $k_{TMD}$ . The equivalent damping coefficients for each DOF are:  $d_B$ ,  $d_T$  and  $d_{TMD}$ .

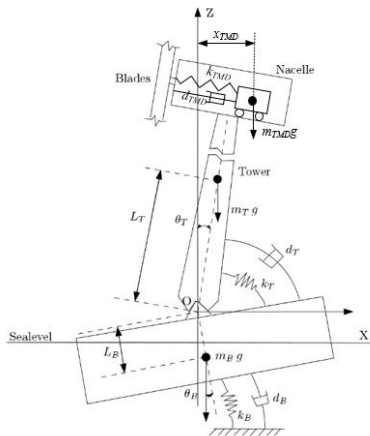


Figure 1. Structural model of the barge-type wind turbine with a TMD

Table 1. FWOT parameters (He et al. [8] and Jonkman [12]).

Parameter	Nomenclature	Value	
Platform Moment of Inertia	$I_B$	1.98E+8	kg·m <sup>2</sup>
Tower Moment of Inertia	$I_T$	2.83E+9	kg·m <sup>2</sup>
Platform Center of Mass Height	$L_B$	0.2818	m
Tower Center of Mass Height	$L_T$	64.00	m
TMD Height	$L_{TMD}$	92.00	m
Platform Mass	$m_B$	5.452E+6	kg
Tower Mass	$m_T$	5.5598E+5	kg
Platform Rotational Spring Value	$k_B$	1.78E+9	N·m/rad
Tower Rotational Spring Value	$k_T$	1.29E+10	N·m/rad
Gravitation Acceleration	$g$	9.78	m/s <sup>2</sup>

The Hamilton's Principle is used to derive the equations of motion of the FWOT-TMD system:

$$\delta \int_{t_1}^{t_2} [T - (U - W)] dt = 0; \quad (1)$$

where  $\delta$  is the variational operator,  $T$  is the kinetic energy,  $U$  the elastic potential energy,  $W$  the work done by the external loads, and  $t_1$  and  $t_2$  are initial and final times.

The kinetic and elastic potential energy expressions are, respectively, equal to:

$$T = \frac{1}{2}I_B \left(\frac{d\theta_B}{dt}\right)^2 + \frac{1}{2}I_T \left(\frac{d\theta_T}{dt}\right)^2 + \frac{1}{2}m_{TMD} \left[\frac{d}{dt}\left(\frac{x_{TMD}}{\cos(\theta_T)}\right)\right]^2; \quad (2)$$

$$U = \frac{1}{2}k_B\theta_B^2 + \frac{1}{2}k_T(\theta_B - \theta_T)^2 + \frac{1}{2}k_{TMD} \left(\frac{x_{TMD}}{\cos(\theta_T)} - L_{TMD}\tan(\theta_T)\right)^2; \quad (3)$$

where  $I_B$  and  $I_T$  are, respectively, the central moments of inertia of the barge and the tower.

The work done by the weight of tower and barge is given by:

$$W = m_B g L_B (1 - \cos(\theta_B)) - m_T g L_T (1 - \cos(\theta_T)) - m_{TMD} g x_{TMD} \tan(\theta_T); \quad (4)$$

where  $g$  is the gravitational acceleration.

The TMD parameters are given for the following relations:

$$m_{TMD} = \mu m_T; \quad (5)$$

$$k_{TMD} = \left(\frac{\omega_{01}}{1+\mu}\right)^2 \mu m_T; \quad (6)$$

$$d_{TMD} = 2\xi \mu m_T \left(\frac{\omega_{01}}{1+\mu}\right); \quad (7)$$

where  $\mu$  is the tuning mass ratio,  $\omega_{01}$  is the first natural frequency of the uncontrolled system and  $\xi$  is the damping ratio.

The equations of motion are obtained by substituting eqs. (2) - (7) into eq. (1) and by applying the variational techniques. The resulted equations are rewritten as Hamilton's type equations using the Cramer's rule. As a first nonlinear approximated analysis, it is common to expand the nonlinear equations of motion in Taylor's series up to third degree terms. The use of the parameters listed on Table 1 and  $\mu=1\%$  results in the following approximated free-undamped equations of motion:

$$\ddot{\theta}_B + 7.4217\theta_B - 6.5152\theta_T - 0.0013\theta_B^3 = 0; \quad (8)$$

$$\ddot{\theta}_T - 4.5583\theta_B + 4.4397\theta_T - 0.0001x_{TMD} + 0.0263\theta_T^3 - 0.0001x_{TMD}\theta_T^2 = 0; \quad (9)$$

$$\ddot{x}_{TMD} - 34.3136\theta_T + 0.2726x_{TMD} + 10.6089\theta_T^3 - 4.4397x_{TMD}\theta_T^2 + 0.0001\theta_T x_{TMD}^2 + 4.5583\theta_B\theta_T x_{TMD} + 3.0000\dot{x}_{TMD}\dot{\theta}_T\theta_T + 1.0000x_{TMD}\dot{\theta}_T^2 = 0. \quad (10)$$

### 3 Linear modal analysis

The underlying linear problem corresponded to eqs. (8) and (10) and the use of the parameters listed on Table 1 result in the following natural frequencies of vibration for the FWOT:  $\omega_{01}=0.5273$  rad/s (0.0839 Hz) and  $\omega_{02} = 3.4028$  rad/s (0.5416 Hz). The controlled system has three linear modes, whose fundamental frequency, for  $\mu=1\%$ ,  $\omega_1=0.4881$  rad/s (0.0777 Hz) is related to TMD. The towers and barge related frequencies for the controlled system, considering  $\mu=1\%$ , are equal to:  $\omega_2=0.5614$  rad/s (0.0893 Hz), and  $\omega_3 = 3.4028$  rad/s (0.5416 Hz) respectively. The effect of the tuning mass rate,  $\mu$ , on the system natural frequencies could be observed in Fig. 2. The  $\Omega$  parameter, in Fig. 2 stands for the relations  $\omega_1/\omega_{01}$ ;  $\omega_2/\omega_{01}$  and  $\omega_3/\omega_{03}$ . It can be observed from Fig. 2 that the increasing of  $m_{TMD}$  decreases the first natural frequency and increases the second one. The third mode remains practically unchanged, this is expected, since the third frequency is related to the barge platform, which is unaffected by the TMD motions due to its position at the tower's top. The decreasing of the first frequency with the TMD mass increasing is explained, according to Sarkar and Fitzgerald [9], by its impact on the tower's stability. In order to avoid external resonance, the natural frequencies of the FOWT must be located out of the typical wave frequency range, which varies according to Bachynski [16] from 0.04 (0.25 rad/s) to 0.25 Hz (1.57 rad/s). Thus, an external resonance could happen in the vicinity of the first natural frequency of the uncontrolled FWOT. For

the controlled system this resonant spectrum band is much wider due to the tuning and its effect on the system first two frequencies. The TMD's positive effect is due the suppression mechanism that damps the energy out using it to TMD stroke as showed by He et al. [8].

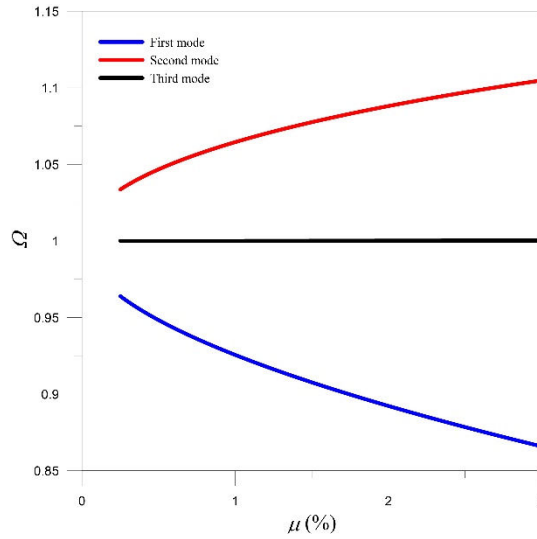


Figure 2. Controlled natural frequencies x TMD mass variation.

#### 4 Nonlinear modal analysis

The invariant manifold approach proposed by Shaw and Pierre [17] is used to derive the nonlinear normal modes (NNMs) of the system. Each NNM, according this approach, corresponds to a motion bounded by a hypersurface in the system phase space. This surface is tangent, at the equilibrium position, to the eigenspace formed by the linear modes of the linearized underlying problem and is given by the solution of the following nonlinear partial differential equations system (Pescheck et al [18]):

$$Q_i(u, v) = \frac{\partial P_i(u, v)}{\partial u} v + \frac{\partial P_i(u, v)}{\partial v} f_1(u, P_2(u, v), v, Q_2(u, v), P_3(u, v), Q_3(u, v)) \quad \forall i = 2, 3; \quad (11)$$

$$f_i(u, P_2(u, v), v, Q_2(u, v), P_3(u, v), Q_3(u, v)) = \frac{\partial Q_i(u, v)}{\partial u} v + \frac{\partial Q_i(u, v)}{\partial v} f_1(u, P_2(u, v), v, Q_2(u, v), P_3(u, v), Q_3(u, v)) \quad \forall i = 2, 3. \quad (12)$$

The system of equations (11) and (12) governs the motion corresponding to a single nonlinear mode, which can be parameterized by the displacement-velocity coordinates pair of a single DOF of the system,  $(u, v)$  which is called the master pair. In this work  $\theta_T = u$  and  $\dot{\theta}_T = v$  are taken as the master pair while the remaining degrees-of-freedom, called slave coordinates, are related to the master pair via constraint equations  $\theta_B = P_2$ ;  $\dot{\theta}_B = Q_2$ ;  $x_{TMD} = P_3$  and  $\dot{x}_{TMD} = Q_3$ . The  $f_1$ ,  $f_2$ , and  $f_3$  functions are from eqs. (8) - (10).

The constraint functions ( $P_2$ ,  $Q_2$ ,  $P_3$  and  $Q_3$ ) determine the invariant manifold geometry for a given NNM and are the solution of eqs. (11) and (12), which in general, do not have an exact closed form solution, except in the presence of certain conditions of symmetry (Pescheck et al [18]): Thus, the asymptotical approximation method proposed by Shaw and Pierre [17] can be used in this case. This is done by assuming a cubic polynomial solution due to the type of non-linearity linearities present in eqs (8) - (10), and analytically solving the system of equations

defined by eqs. (11) and (12). This results in three real solutions for the coefficients of the power series assumed as constraint functions, one for each NNM. Replacing the generalized coordinates of the master and the slave pairs into the equations of motion, the following forced-damped one-degree-of-freedom nonlinear modal oscillators are obtained for the first, second and third NNMs, respectively, taken  $\mu=0.1\%$ :

$$\ddot{u} + 0.2382u + 0.9761\xi\dot{u} - 0.0068u^3 + 1.1015u\dot{u}^2 = 0.0365\Gamma\sin(\omega t); \tag{13}$$

$$\ddot{u} + 0.3151u + 1.1227\xi\dot{u} + 0.0422u^3 + 0.7136u\dot{u}^2 = 0.0365\Gamma\sin(\omega t); \tag{14}$$

$$\ddot{u} + 11.5807u + 6.8061\xi\dot{u} + 0.0119u^3 - 0.0011u\dot{u}^2 = 0.0365\Gamma\sin(\omega t); \tag{15}$$

where  $\Gamma$  is included to facilitate parametric studies and its equal to  $M/M_0$ , where  $M_0$  is the moment caused by the weight of the displaced volume of water corresponded to the motion of the barge draft and  $M$  is the external moment magnitude.

As the resonant response of a structural system occurs at the vicinity of NNM motion (Vakakis et al., [19]), the modal oscillators given by eqs. (13) - (15) can provide useful information about the forced oscillations of the FWOT-TMD system. As a preliminary study an external harmonic moment of amplitude equal to  $M$  and frequency  $\omega$  is used here. Those modal oscillators can be used to describe the behavior of a specific motion corresponding to a NNM, identifying important nonlinear dynamic phenomena and corresponding, also, to a reduction in the order of the problem, which facilitates the nonlinear vibration study of the system. The solution using the modal oscillators concurs with the numerical integration of the nonlinear equations of motion up to amplitudes of 1.0 rad for both modes according to a preliminary study conducted by the authors of the uncontrolled system [11].

The resonance curves can be obtained using the harmonic balance method and are shown for the first and second modes in Fig. 3 (a) and for the third mode in Fig. 3 (b) using a dimensionless frequency parameter defined as  $\Omega=\omega/\omega_{01}$ . From Fig. 3 it is possible to observe a hardening behavior, and both jump and hysteresis phenomena, indicating that the forced response of FOWT is bistable, with two possible amplitudes of motion for each frequency, for some set of damping factor and amplitude of external moment values. This is due to two saddle-node bifurcations separating the stable and unstable branches along the nonlinear resonance curves. By comparing the controlled system with the uncontrolled case, which first mode is included on Figure 3 (a), one can observe the fore-aft suppression (distance between the curves peaks) due to the TMD action. The controlled system third mode, which corresponds to the uncontrolled system second one, remains practically unchanged in respect to  $\mu$  values variation, in accordance to the linear modal analysis results.

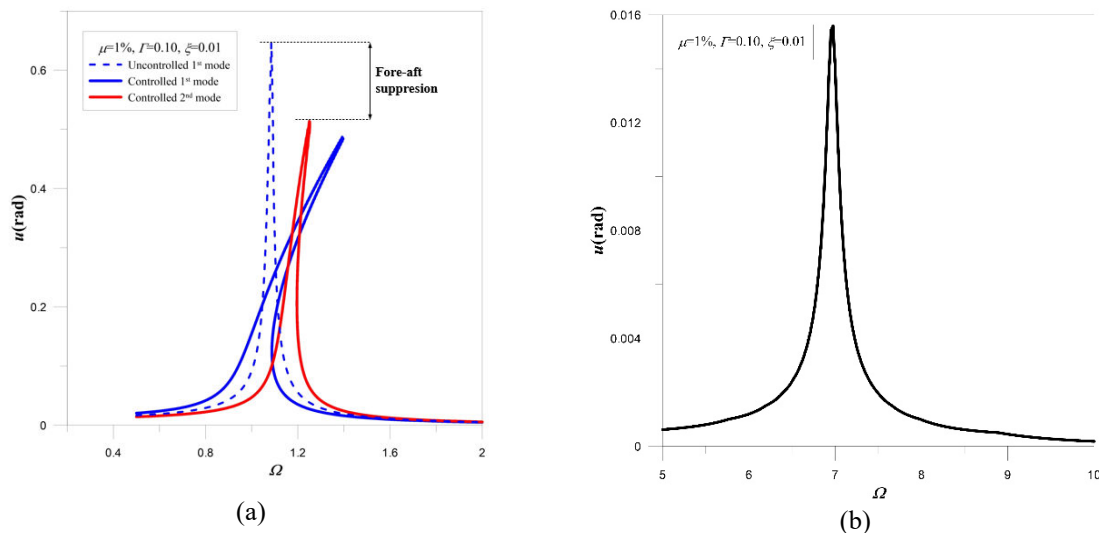


Figure 3. Resonances curves: (a) 1<sup>st</sup> and 2<sup>nd</sup> NNMs; (b) 3<sup>rd</sup> NNM.

The suppression rate,  $\eta$ , depends upon the TMD parameters, mainly the  $\mu$  ratio, whose values is about 0.25% to 2.5% in current engineering structures according to He and co-workers [8]. Smaller  $\mu$  values lead to higher peaks for the 2<sup>nd</sup> mode (while the 1<sup>st</sup> mode peak gets smaller). On the other hand, larger  $\mu$  values lead to higher

peaks for the 1<sup>st</sup> mode (while the 2<sup>nd</sup> mode peak gets smaller). The optimum mass ratio values,  $\mu_{op}$ , which corresponds to equal first and second peaks, can be determined using the 1-DOF oscillators given by eqs. (13) and (14) and the balance harmonic method. The obtained optimum  $\mu$  values are listed on Table 2 for some  $\Gamma$  and  $\xi$  values.

Table 2. Optimum  $\mu$  values.

$\xi = 0.090$			$\Gamma = 0.10$		
$\Gamma$	$\mu_{op}$ (%)	$\eta$ (%)	$\xi$	$\mu_{op}$ (%)	$\eta$ (%)
0.08	0.86	-16.85	0.050	2.63	-33.7
0.09	1.03	-19.16	0.075	1.55	-25.11
0.10	1.02	-21.29	0.090	1.20	-21.29
0.15	2.09	-29.87	0.100	1.03	-19.16
0.20	2.65	-36.28	0.150	0.55	-11.86
0.25	3.86	-40.15	-	-	-

The maximum obtained  $\eta$  value for the parameters set investigated is about -40%, confirming the positive effects of the TMD. However this maximum value is minor compared to the -60% obtained by He et al. [8] for the linear analysis. From Table 2 results one can observe the suppression rate increases to larger values of external force magnitude and smaller damping factors. However smaller  $\xi$  and larger  $\Gamma$  values demand larger TMD masses to optimize its performance. FWOT stability is highly affected by the TMD mass. This fact results that the nonlinear observed phenomena get more prominence with the  $\mu_{op}$  increasing. Since the jump phenomenon is very sensitive to the damping factor and in a smaller degree to the external moment magnitude, the richer nonlinearity due to larger  $\mu_{op}$  values can be confirmed by the minimum required damping factor ( $\xi_{min}$ ) and the maximum allowable moment magnitude ( $\Gamma_{max}$ ) values in order to avoid jump phenomenon (and the included unstable solutions) as showed on Table 3, which also shows those parameters values for the uncontrolled system. It can be observed from Table 3 results that the TMD use greatly reduces the domain of possible  $\xi$  and  $\Gamma$  parameters whose unstable solutions do not exist. This domain gets smaller with the increasing of TMD mass ratio.

Table 3. Damping factor and force magnitude values to avoid jumping phenomenon.

$\mu_{op}$ (%)	$\xi$	$\Gamma$	Controlled system		Uncontrolled system	
			$\xi_{min}$	$\Gamma_{max}$	$\xi_{min}$	$\Gamma_{max}$
0.55	0.015	0.10	0.059	0.012	0.011	0.157
0.86	0.090	0.08	0.052	0.006	0.010	0.073
1.03	0.010	0.10	0.060	0.007	0.011	0.085
1.20	0.090	0.10	0.061	0.006	0.011	0.073
1.55	0.075	0.10	0.062	0.004	0.011	0.075
2.09	0.090	0.15	0.083	0.005	0.015	0.073
2.63	0.050	0.10	0.065	0.004	0.011	0.030
2.65	0.090	0.20	0.102	0.005	0.018	0.073
3.86	0.090	0.25	0.126	0.004	0.020	0.073

## 5 Conclusions

According to the results of this work it is possible to obtain important features of the nonlinear dynamic behavior of a barge-type FWOT controlled by a TMD using the nonlinear normal modes theory. The TMD performance was investigated in the nonlinear analysis. A maximum vibration suppression rate equal to -40% was observed for the studied cases. The addition of the TMD enriches the system nonlinearities, mainly for the first and second modes of the system. As the TMD mass gets larger the system parameters domain of instability also becomes larger. Such instability, linked to jumps between the coexisting solutions in an evolving dynamic environment which can be very harmful to the Barge FOWT structure.

**Acknowledgements.** The authors would like to thank the Departamento de Construção Civil da UFPR, the Programa de Pós-Graduação em Engenharia Civil (PPGEC/UFPR) and the Centro de Estudos em Engenharia Civil (CESEC/ UFPR) for their support.

**Authorship statement.** The authors hereby confirm that they are the sole liable persons responsible for the authorship of this work, and that all material that has been herein included as part of the present paper is either the property (and authorship) of the authors, or has the permission of the owners to be included here.

## References

- [1] I. F. A. A. Vis and E. Ursavas, "Assessment approaches to logistics for offshore wind energy installation," *Sustain. Energy Technol. Assessments*, vol. 14, pp. 80–91, Apr. 2016, doi: <https://doi.org/10.1016/j.seta.2016.02.001>.
- [2] Y. Hu, J. Wang, M. Z. Q. Q. Chen, Z. Li, and Y. Sun, "Load mitigation for a barge-type floating offshore wind turbine via inerter-based passive structural control," *Eng. Struct.*, vol. 177, pp. 198–209, Dec. 2018, doi: <https://doi.org/10.1016/j.engstruct.2018.09.063>.
- [3] M. Collu, A. J. Kolios, A. Chahardehi, and F. Brennan, "A COMPARISON BETWEEN THE PRELIMINARY DESIGN STUDIES OF A FIXED AND A FLOATING SUPPORT STRUCTURE FOR A 5 MW OFFSHORE WIND TURBINE IN THE NORTH SEA," *Mar. OFFSHORE Renew. ENERGY - Dev. Wind. Wave, Tidal Curr. Technol.*, pp. 63–74, 2010.
- [4] H. Zuo, K. Bi, and H. Hao, "A state-of-the-art review on the vibration mitigation of wind turbines," *Renew. Sustain. Energy Rev.*, vol. 121, p. 19, Apr. 2020, doi: [10.1016/j.rser.2020.109710](https://doi.org/10.1016/j.rser.2020.109710).
- [5] X. Li and H. Gao, "Load mitigation for a floating wind turbine via generalized  $h_{\infty}$  structural control," *IEEE Trans. Ind. Electron.*, vol. 63, no. 1, pp. 332–342, 2016, doi: [10.1109/TIE.2015.2465894](https://doi.org/10.1109/TIE.2015.2465894).
- [6] G. M. Stewart, "Load Reduction of Floating Wind Turbines using Tuned Mass Dampers," 2014.
- [7] S. Xie, X. Jin, J. He, and C. Zhang, "Structural responses suppression for a barge-type floating wind turbine with a platform-based TMD," *IET Renew. Power Gener.*, vol. 13, no. 13, pp. 2473–2479, 2019, doi: [10.1049/iet-rpg.2018.6054](https://doi.org/10.1049/iet-rpg.2018.6054).
- [8] E.-M. He, Y.-Q. Hu, and Y. Zhang, "Optimization design of tuned mass damper for vibration suppression of a barge-type offshore floating wind turbine," *Proc. Inst. Mech. Eng. Part M J. Eng. Marit. Environ.*, vol. 231, no. 1, pp. 302–315, 2017, doi: [10.1177/1475090216642466](https://doi.org/10.1177/1475090216642466).
- [9] S. Sarkar and B. Fitzgerald, "Vibration control of spar-type floating offshore wind turbine towers using a tuned mass damper-inerter," *Struct. Control Heal. Monit.*, vol. 27, no. 1, 2020, doi: [10.1002/stc.2471](https://doi.org/10.1002/stc.2471).
- [10] E. Gavassoni, P. Batista Gonçalves, D. De Mesquita Roehl, P. B. Gonçalves, and D. de M. Roehl, "Nonlinear vibration modes of an offshore articulated tower," *Ocean Eng.*, vol. 109, pp. 226–242, Nov. 2015, doi: [10.1016/j.oceaneng.2015.08.028](https://doi.org/10.1016/j.oceaneng.2015.08.028).
- [11] E. Gavassoni and P. D. G. Zwierzikowski, "The nonlinear modal analysis of a barge-type offshore wind turbine," 2020.
- [12] J. M. Jonkman, "Dynamics modeling and loads analysis of an offshore floating wind turbine," *Natl. Renew. Energy Lab. NREL/TP-500-41958*, vol. 68, no. November, p. 233, 2007, [Online]. Available: <http://www.nrel.gov/docs/fy08osti/41958.pdf>.
- [13] J. Jonkman, S. Butterfield, W. Musial, and G. Scott, "Definition of a 5-MW Reference Wind Turbine for Offshore System Development, NREL Technical Report No. TP-500-38060," *NREL*, no. February, Feb. 2009, doi: [10.2172/947422](https://doi.org/10.2172/947422).
- [14] J. Yang, E. M. He, and Y. Q. Hu, "Dynamic modeling and vibration suppression for an offshore wind turbine with a tuned mass damper in floating platform," *Appl. Ocean Res.*, vol. 83, pp. 21–29, Feb. 2019, doi: [10.1016/J.APOR.2018.08.021](https://doi.org/10.1016/J.APOR.2018.08.021).
- [15] H. Sun, L. Zuo, X. Wang, J. Peng, and W. Wang, "Exact H 2 optimal solutions to inerter-based isolation systems for building structures," *Struct. Control Heal. Monit.*, vol. 26, no. 6, 2019, doi: [10.1002/stc.2357](https://doi.org/10.1002/stc.2357).
- [16] E. E. Bachynski, "Fixed and Floating Offshore Wind Turbine Support Structures," *Offshore Wind Energy Technology*. John Wiley & Sons, pp. 103–142, 2018, doi: [10.1002/9781119097808.ch4](https://doi.org/10.1002/9781119097808.ch4).
- [17] S. Shaw and C. Pierre, "Non-linear normal modes and invariant manifolds," *J. Sound Vib.*, vol. 150, no. 1, pp. 170–173, 1991.
- [18] E. Pescheck *et al.*, "Non-linear modal analysis of structural systems using multi-mode invariant manifolds," *Nonlinear Dyn.*, vol. 25, no. 734, pp. 183–205, 1994, doi: [10.2514/6.1994-1672](https://doi.org/10.2514/6.1994-1672).
- [19] A. F. Vakakis, L. I. Manevitch, Y. V. Mikhlin, V. N. Pilipchuk, and A. A. Zevin, *Normal Modes and Localization in Nonlinear Systems*. Wiley, 1996.